Telluride mineralization at Ashanti gold mine, Ghana

R. J. BOWELL, R. P. FOSTER

Department of Geology, University of Southampton, Southampton SO9 5NH

AND

C. J. STANLEY

Department of Mineralogy, The Natural History Museum, Cromwell Road, London SW7 5BD

Abstract

Gold mineralization at the Ashanti Mine occurs in shear zones which are second-order components of a major transcrustal shear zone. However, gold-rich telluride mineralization in veins in the hangingwall of the Obuasi ore zone at Ashanti appears to have post-dated development of the major gold-bearing shear zone. Complex assemblages of goethite, chalcocite, coloradoite, calaverite, sylvanite, kostovite, petzite, stutzite, hessite, altaite, rickardite, weissite and henryite were succeeded by a relatively simple assemblage of altaite–petzite–hessite ± sylvanite ± coloradoite. Precipitation occurred over a temperature range of approximately 220°C to 165°C from a CO_2-bearing, low salinity (<5 wt.% NaCl equiv.) fluid under conditions of high f_{O_2} and high f_{Te_2}/f_{S_2}. Replacement of earlier gold–sulphide mineralization is indicated.

The fluids were introduced during late activation of the Obuasi shear zone, which evolved during the *c.*2000 Ma Eburnean tectonothermal event that marked the onset of cratonization of the West African shield. The localized and time-specific distribution of the telluride mineralization may be indicative of a late influx of tellurium-rich fluid linked to emplacement of a synorogenic, Cape Coast-type granitoid intrusion.

KEYWORDS: telluride, gold, mineralization, Ashanti, Ghana.

Introduction

THE Ashanti Goldfields Concession is situated at Obuasi, 160 km north–west of Accra, in the Ashanti region of Ghana (Fig. 1). It has been worked continuously for nearly 90 years and in the period between 1898 and September 1986 the mine produced 584 t (18.7 Moz) of gold from 25.9 million tonnes of ore milled, giving an average recovery grade of 22.5 g/t (Cappendell, 1987). Production during 1988 totalled 9695 kg (311 721 oz) of gold (Suttill, 1989).

The mine concession lies on a regional shear zone system which extends for a distance of 195 km south-west of Obuasi and continues for a further 65 km to the north-east. The nature and setting of this shear zone system is briefly described but the main emphasis is placed on recording, for the first time, the occurrence of precious and base metal telluride mineralization which comprises a small but important component of the mineralization at Ashanti.

Geology of south-west Ghana

Much of southern and south-western Ghana is underlain by late Archaean and early Proterozoic rocks of the West African craton (Fig. 1). This supracrustal sequence is dominated by the 10000–15000 m of sedimentary and volcanic rocks of the Birimian, regarded as a 'Series' by Kesse (1985) but defined as a Supergroup by Hirdes *et al.* (1988*a*) and Leube *et al.* (1990). The Lower Birimian comprises phyllites, greywackes, and tuffs which pass conformably upwards into basaltic and andesitic volcanics with minor felsic flows and intercalated clastic sediments of the Upper Birimian. The whole sequence was tightly folded along NNE-trending axes and metamorphosed to greenschist and, in places, almandine-amphibo-

Mineralogical Magazine, December 1990, Vol. 54, pp. 617–627

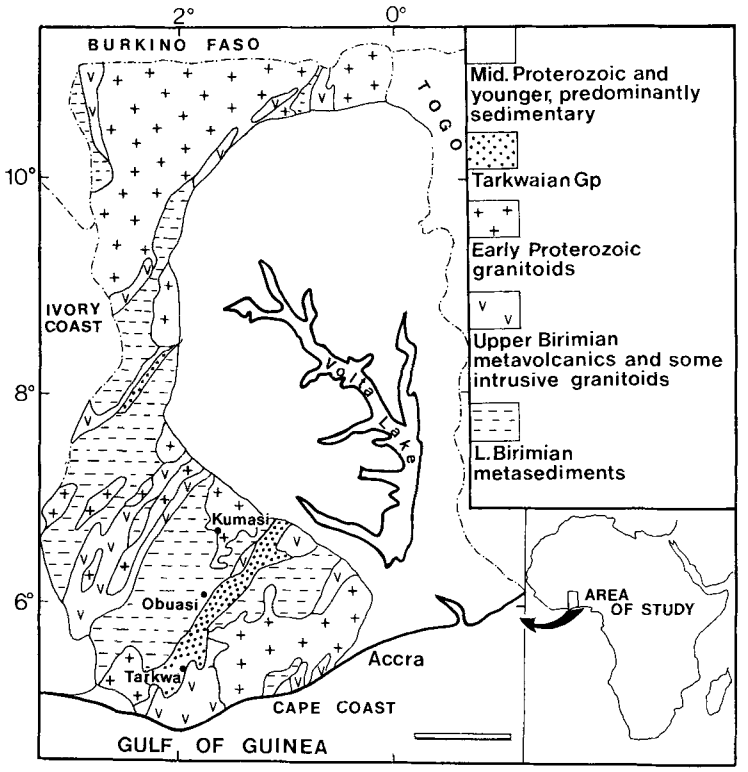

FIG. 1. Geology of Ghana (modified after Kesse, 1984).

lite facies during the *c.*2000 Ma Eburnean tectonothermal event (Wright *et al.*, 1985).

An angular unconformity separates the Birimian supracrustal rocks from the overlying shallow-water, fluviatile sediments of the Tarkwaian Group, which includes the quartz-pebble conglomerates which are being mined for gold in the Tarkwa area (Kesse, 1985; Hirdes *et al.*, 1988*b*).

The upper Birimian volcanics have yielded a Rb/Sr radiometric age of 2166 ± 66 Ma (Hirdes *et al.*, 1988*a*; Leube *et al.*, 1990) and the succeeding Tarkwaian sedimentation has been constrained to between 2081 ± 25 Ma and 1968 ± 49 Ma by Rb/Sr radiometric studies (Hirdes *et al.*, 1988*b*). Two suites of granitoids occur within the Birimian sequence but they appear to pre-date the Tarkwaian metasediments (Wright *et al.*, 1985). The earlier, granodiorite-dominated Cape Coast-type intrusions generally show a pronounced fabric and were emplaced during the Eburnean orogeny, which overprinted Birimian and Tarkwaian Group rocks at *c.*2.0–1.9 Ga. The tonalites of the Dixcove suite, however, are discordant, mostly unfoliated, and were intruded after the Eburnean event (Kesse, 1985; Wright *et al.*, 1985; Hirdes *et al.*, 1988*a*).

Geology of the Ashanti Concession

The ill-defined contact between Lower and Upper Birimian supracrustal rocks appears to have been the general locus for much of the lode gold mineralization in western Ghana (Kesse, 1985; Milesi *et al.*, 1988). Within the Ashanti concession, mineralized shear zones occur in tightly folded Lower Birimian metasedimentary rocks close to the contact with the more competent metamorphosed and metasomatically altered Upper Birimian volcanics to the east (Fig. 2). Birimian metasediments are dominated by phyllites containing variable amounts of carbonaceous matter and intercalated with arenaceous rocks, tuffs, and chlorite–carbonate–sericite schists of uncertain ancestry.

The strata strike approximately N15°E and dip 60–90°NNW (Fig. 2) and at least two phases of deformation can be recognized. The earlier F_1 folds commonly plunge at approximately 30° to-

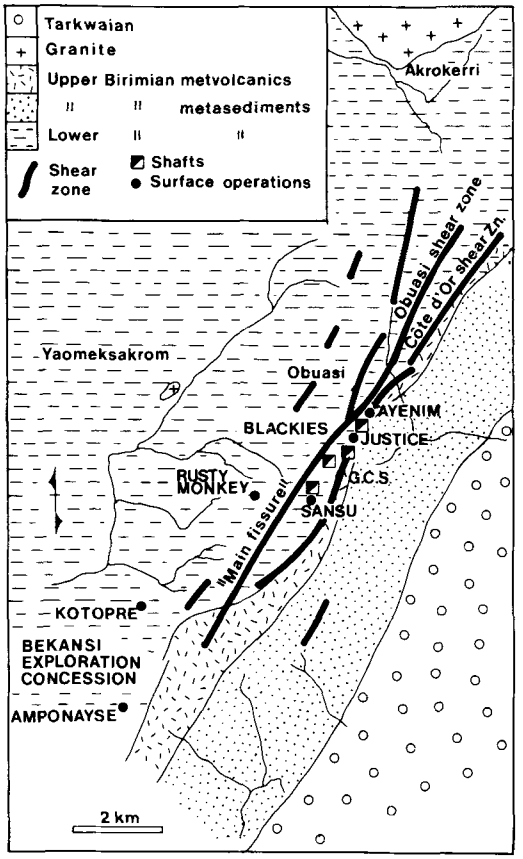

FIG. 2. Geology of a part of the Ashanti Mine Concession area (after Amanor *et al.*, 1978).

wards 060° whereas the F_2 folds are localized and less well-developed (Junner, 1932). A penetrative S_1 cleavage is developed in the axial zones of the F_1 folds and appears to have been an important locus of shearing.

The regional metamorphism in the Ashanti concession is of lower greenschist facies, although, widespread metasomatism has led to overprinting with an assemblage of iron-rich carbonate + sericite + chlorite + pyrite. A granitoid intrusion some 8 km north of Obuasi exhibits a well-developed fabric and is probably a member of the synorogenic Cape Coast suite.

Ore zones

The ore-bearing shear zones in the Ashanti concession represent second-order structures within the 260 km-long NNE-trending, main shear zone which is a major transcrustal dislocation. Three significant mineralized shears, the Cote D'Or, Obuasi, and Ashanti (in the northern section), converge at depth to form the 'Main Reef Fissure' (Fig. 3). The overall appearance (Fig. 3) resembles a flower structure (see Harding, 1985) but the sense of movement is complex with evidence for both strike-slip and dip-slip (normal and reverse) components.

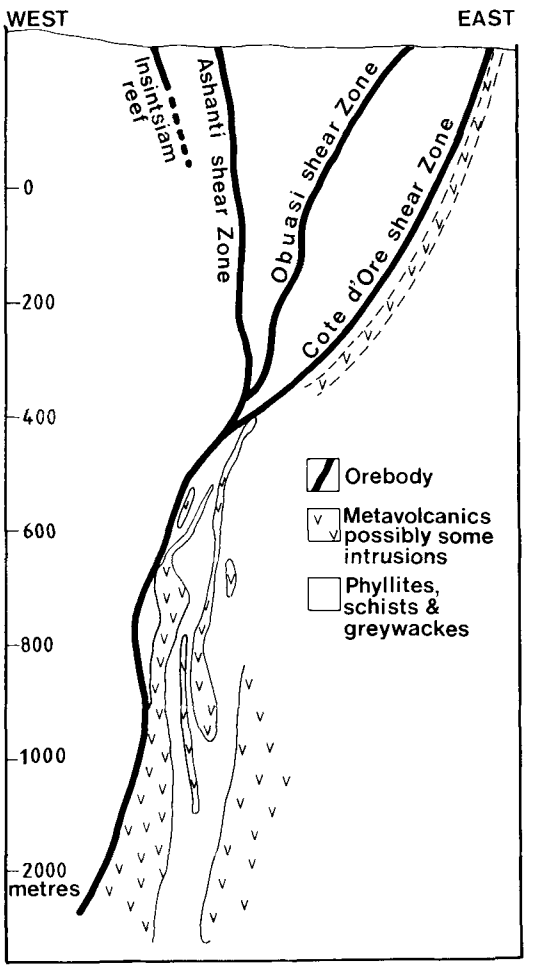

FIG. 3. West–east cross-section of the Ashanti ore zones at the Ashanti shaft (modified after Amanor, 1979).

The auriferous ore occurs both as massive and ribboned quartz veins 1–3 m in thickness, occasionally to 15 m, and as disseminated sulphides and sulpharsenides (predominantly arsenopyrite) in anastomosing ductile shear zones hosted by car-

Table 1 Phases of mineralization in the main ore zone ("Main Reef Fissure"), Ashanti.

Stage	Quartz vein types	Structural location	Ore mineralogy
I	Massive smokey blue-grey quartz	Main shear zone and small vein-offshoots in the hangingwall	Arsenopyrite, gold, sphalerite galena, chalcopyrite, pyrite, tetrahedrite, bournonite, bornite, pyrrhotite, alabandite
IIa	Milky white quartz vein often ribboned	Infills fractures in the stage I quartz and occupies vein-offshoots in the hangingwall	Arsenopyrite, gold, sphalerite, galena, chalcopyrite, pyrite, stibnite, tetrahedrite, bournonite, bornite, pyrrhotite, alabandite, goethite, chalcocite, coloradoite, altaite, hematite, petzite, hessite, sylvanite, calaverite, kostovite, rickardite, stutzite, henryite, weissite
IIb	Calcite-quartz veinlets	Confined to cross-cutting telluride pods in stage IIa quartz	Altaite, gold, petzite, sylvanite, hessite
III	Barren quartz vein with up to 20% calcite	Veins and stringers in the footwall and hangingwall	-
IV	Barren quartz vein; no calcite	Veins and stringers in the footwall and hangingwall	-

bonaceous phyllites and metabasalts. The ore zones have been mined over a discontinuous strike length of 8 km and down to a maximum depth, in the northern section, of 1650 m. The gold is confined to well-defined ore shoots which plunge at 45° towards the north in the northern section and more steeply in the central part of the mined area.

The veins occupy dilational zones which were particularly well developed at inflection points (changes of strike and dip) in the major ductile–brittle shear zone and also at points of intersection of shears (Gyapong, 1980). Four generations of quartz veins are recognizable in the mine (Table 1): an early, massive, smokey blue–grey quartz (stage I) which is the dominant component and hosts most of the gold; ribboned white quartz (stage II) which has partly replaced the blue–grey quartz and in places contains particularly high concentrations of gold; and later quartz–calcite (stage III) and quartz (stage IV) veins which tend to transect the earlier phases of mineralization and are usually devoid of gold.

Common minerals in the gold-bearing quartz veins are arsenopyrite, sphalerite, galena, chalcopyrite, gold, ferroan calcite and sericite. Minor minerals include pyrite, stibnite, pyrrhotite, alabandite, bornite, tetrahedrite, tourmaline and hydrothermal graphite (Junner, 1932; Wilson, 1972*b*; Amanor *et al.*, 1978; Amanor, 1979; Gyapong, 1980). A similar mineral association is evident in the shear-hosted disseminated ore but the sulphides and gold are confined predominantly to the altered wallrocks. Native gold is less common in the disseminated ore, with most of the gold occurring as microscopic inclusions in sulphides, chiefly arsenopyrite. Base-metal sulphides are also rare in the disseminated ore, with arsenopyrite, pyrite and pyrrhotite being dominant.

The wallrocks often contain finely divided amorphous carbon (Wilson, 1972*a*) and these rocks have been intensely sheared. The present study confirmed that wallrock alteration is characterized by sulphidation, sericitization, and carbonatization accompanied by apparent increases in Al_2O_3, K_2O, CO_2, CaO, MgO, FeO and MnO. Silicification is locally important and has generated silicified phyllites and tuffs which in places host significant amounts of disseminated gold-sulphide ore. Albitization has been reported by Junner (1932) and Wilson (1972*b*).

Samples of vein were collected from the George Cappendell Shaft section of the mine (hereafter referred to as GCS; Fig. 2). Examination of the samples confirmed the earlier mineralogical investigations, although alabandite was noted only as inclusions in sphalerite. Bournonite, previously unreported from Ashanti, was also seen and, together with tetrahedrite, occurred as inter-

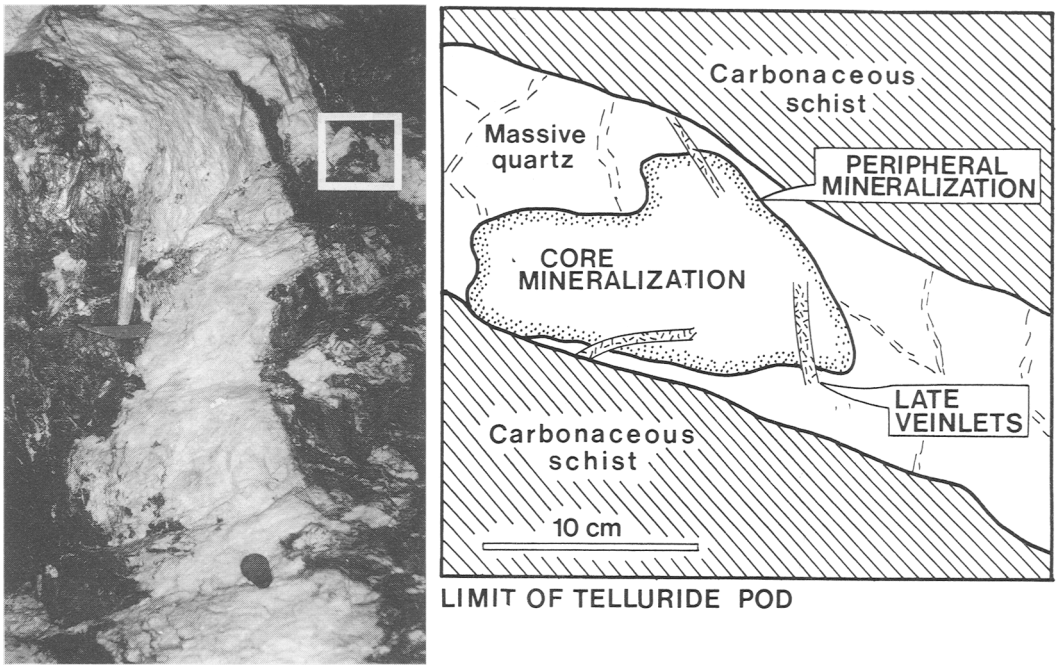

FIG. 4. Pod of telluride mineralization (top right and adjoining sketch) in a hangingwall quartz vein adjacent to the main Obuasi orebody, GCS section, 12.5 level, cross-cut 286. Shaft of hammer is 30 cm long.

growths with coarse gold (grains up to 5 mm in size).

Telluride mineralization

The telluride minerals, accompanied by a contemporaneous hypogene assemblage of hematite + goethite + chalcocite + calcite, occur as podiform aggregates in veins of milky white quartz and ferroan calcite located in the immediate hangingwall of the main GCS orebody and often representing offshoots of the main orebody (Fig. 4).

A total of eleven telluride minerals have been identified by microscopy and electron microprobe studies (Table 2) but of these only four—altaite, coloradoite, petzite, and hessite—have been observed as macroscopic grains. The tellurides occur as complex aggregates with white quartz (stage IIa) infilling fractures in the blue–grey quartz veins. In the five podiform occurrences observed to date, the tellurides show a crudely zoned distribution (Fig. 4) passing outwards from a core of coloradoite–goethite–chalcocite–rich mineralization along strike and towards the vein walls into a peripheral assemblage dominated by altaite. In places, the core and peripheral mineralization are cross-cut by late quartz–calcite veinlets containing coarse gold and minor telluride minerals (stage IIb). These different styles of mineralization are considered separately below.

Core mineralization (IIa). The central parts of the telluride-rich pods range from metallic to earthy brown in colour, reflecting the relative abundances of coloradoite and goethite. Chalcocite is also an important constituent of the core mineralization and the three minerals are accompanied by minor hematite, chalcopyrite, bornite, gold- and silver-bearing tellurides, and altaite. Within the larger grains (1–5 mm) of chalcocite and coloradoite are complex intergrowths of rickardite, weissite, henryite, stutzite, hessite, and petzite (Fig. 5). Henryite is a rare copper–silver telluride ($Cu_2Ag_3Te_4$; Criddle *et al.*, 1983), for which this is only the second recorded occurrence. Sylvanite occurs as inclusions in the chalcocite.

Symplectic intergrowths, developed in intercrystalline areas between larger (1–5 mm) subhedral crystals of goethite, comprise calaverite, sylvanite, kostovite, and petzite intergrown with goethite and hematite (Fig. 6). These intergrowths enclose and in places have replaced grains of native gold (Fig. 7). Discrete grains of chalco-

Table 2 Electron microprobe analytical data for tellurides and gold[1] from Ashanti Mine, Ghana

MINERAL	Au	Ag	Te	Cu	Pb	Hg	Bi	Total	Sample and location
	all in weight %								
GOLD	90.57	8.84	0.06	0.07	-	-	-	99.54	RB6, free grain in quartz
	89.88	9.94	0.01	0.08	-	-	-	100.13	RB43, free grain in calcite
	88.89	10.09	0.01	0.10	-	-	-	99.09	RB41, inclusion in altaite
	88.60	11.10	0.00	0.08	-	-	-	99.78	RB38, free grain associated with petzite
PETZITE Ag_3AuTe_2	13.84	50.43	36.43	0.02	-	-	-	100.74	RB6, free grain in quartz, probe-sensitive
	25.84	41.70	32.77	0.05	-	-	-	99.95	RB6, cut by sylvanite-hessite veinlet
	25.54	40.03	33.60	0.07	-	-	-	99.46	RB43, free grain in calcite
	25.60	50.95	33.60	0.07	-	-	-	100.22	E1277, free grain next to coloradoite
SYLVANITE $AuAgTe_4$	24.10	12.40	62.50	0.30	-	-	-	99.30	RB6, in veinlet cutting petzite
	23.70	13.06	62.16	0.25	-	-	-	99.17	RB43, inclusion in petzite
	24.60	11.12	62.55	1.17	-	-	-	99.44	E1277, symplectic intergrowth with goethite
	24.69	11.06	62.40	1.07	-	-	-	99.30	RB59, inclusion in hessite
CALAVERITE $AuTe_2$	43.00	0.35	56.45	0.14	-	-	-	100.94	RB41, symplectic intergrowth with goethite
	40.95	0.38	57.59	0.20	-	-	-	99.12	E1277, symplectic intergrowth of goethite and sylvanite
KOSTOVITE $AuCuTe_4$	24.47	0.79	66.08	9.07	-	-	-	100.41	RB41, symplectic intergrowth of sylvanite and goethite
	24.36	0.71	66.04	9.34	-	-	-	100.45	RB59, inclusion in sylvanite
	24.38	0.72	66.04	9.20	-	-	-	100.34	E1277, symplectic intergrowth with sylvanite and goethite replacing gold
RICKARDITE $Cu_{2-X}Te$	-	0.22	60.09	39.52	-	-	-	99.83	E1277, inclusion in chalcocite
	-	1.24	60.17	39.50	-	-	-	100.91	RB41, inclusion in hessite
WEISSITE Cu_2Te	-	0.94	55.97	41.15	-	-	-	99.06	RB41, inclusion in chalcocite
	-	0.72	54.90	42.80	-	-	-	98.42	E1277, inclusion in chalcocite
HENRYITE $Cu_{3.77}Ag_{3.01}Te_4$	-	29.44	48.40	22.66	-	-	-	100.63	E1277, inclusion in chalcocite
	-	28.65	48.14	22.19	-	-	-	98.98	RB41, inclusion in hessite
HESSITE Ag_2Te	0.12	59.40	39.89	0.93	0.00	-	0.00	100.34	RB41, hosts henryite
	0.04	61.20	37.86	0.07	0.53	-	0.00	99.70	RB6, in veinlet cutting petzite
	0.01	60.19	37.73	0.72	0.00	-	0.08	98.73	E1277, inclusion in chalcocite
	0.07	60.19	39.23	0.02	0.77	-	0.00	100.28	RB43, free grain in calcite
STUTZITE Ag_5Te_3	-	56.26	41.88	0.69	-	1.00	-	99.83	RB38, inclusion in coloradoite
	-	56.78	41.27	1.27	-	0.60	-	99.92	E1277, inclusion in chalcocite
ALTAITE PbTe	-	0.03	37.35	0.04	61.53	0.00	0.16	99.05	RB6, free grain
	-	0.02	38.55	0.10	61.43	0.14	0.08	100.32	RB52, free grain
	-	0.35	38.79	0.02	61.63	0.02	0.08	100.89	E1277, large grain hosts tellurides and chalcocite
COLORADOITE HgTe	-	0.00	39.03	0.14	-	61.53	-	100.70	RB41, large grain hosts other tellurides
	-	0.05	38.82	0.14	-	61.95	-	100.16	E1277, large grain hosts other tellurides

All microprobe analysis by Cambridge Instruments Microscan IX
accelerating voltage of 20kV
beam current of 2.50×10^{-8}A on the Faraday Cage
standards: pure elements and PbTe, HgS
radiations measured: Au-Lα,Au-Mα,Ag-Lα,Cu-Lα,Te-Lα,Pb-Mα,Hg-Lα,Bi-Mα

[1] Data selected to illustrate complete range of chemical composition for each mineral analysed. Some petzite grains showed probe sensitivity with loss of gold and consequent enrichment of silver.

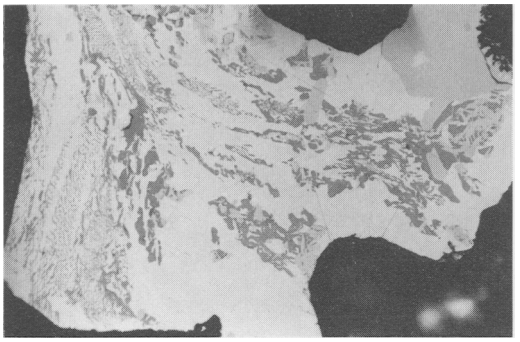

FIG. 5. Photomicrographs of chalcocite (white) hosting chalcopyrite (light grey), bornite (dark grey), and symplectic intergrowths of rickardite, sylvanite and henryite. Field of view = 340 μm across. GCS section, 12.5 level, cross-cut 286.

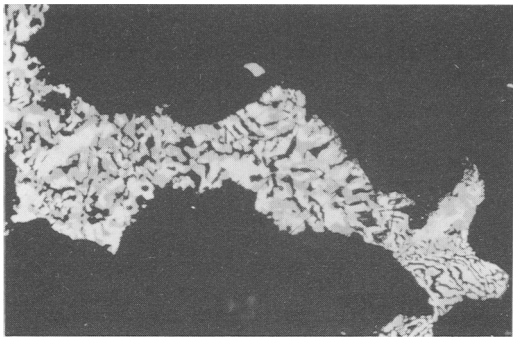

FIG. 6. Photomicrograph of symplectic intergrowth between sylvanite (pale grey), calaverite (white) and goethite (black). Field of view = 340 μm across. GCS section, 12.5 level, cross-cut 286.

pyrite are present but are partially replaced by bornite, which in turn has been replaced by chalcocite, goethite, petzite, and the copper-bearing tellurides rickardite, weissite, and henryite.

Arsenopyrite, pyrite, and pyrrhotite are important components of the main vein-type mineralization but they do not occur, either as primary or relict phases, within the goethite–hematite–telluride assemblages. Due to the depth (400 m) of the mineralization and the presence of unoxidized sulphides in this assemblage, the goethite and hematite must be primary hypogene phases and not supergene weathering products.

Peripheral mineralization (IIa). The outer zones of the telluride pods are usually a metallic green colour due to the dominance of altaite. The lead telluride occurs as large anhedral grains from 1–5 mm in size and is accompanied by minor petzite, hessite, and native gold. Like the core mineralization, the altaite-dominated assemblage occupies fractures in the earlier quartz–calcite veins.

Late gold-rich veinlets (IIb). The late cross-cutting veinlets contain relatively abundant altaite, petzite, and visible gold which are intergrown with the quartz and calcite and also occupy cleavage planes in the calcite. Larger grains of petzite, up to 2 mm in size, commonly contain inclusions of altaite, sylvanite, hessite, and coloradoite. Small fractures 0.1–1 mm in width, containing hessite and sylvanite cross-cut some of the larger petzite grains (Fig. 8).

Several generations of white quartz veins transect both the podiform mineralization and late gold-rich veinlets but these are devoid of tellurides and gold.

Fluid Inclusion thermometry

A limited thermometric study of fluid inclusions in the different phases of quartz was undertaken. Two-phase liquid–vapour inclusions in smokey blue–grey quartz (stage I) of the main GCS orebody yielded temperatures of homogenization (T_h) of 340–267°C (Fig. 9*a*). Single-phase inclusions up to 5 μm in size were also noted, some 30% being filled with CO_2. Identical quartz (stage I), occurring as ill-defined patches enclosed by white quartz (stage II*a*) within the telluride-rich pods, gave a T_h range of 320–270°C (Fig. 9*b*) and appear to represent relicts of the early gold–

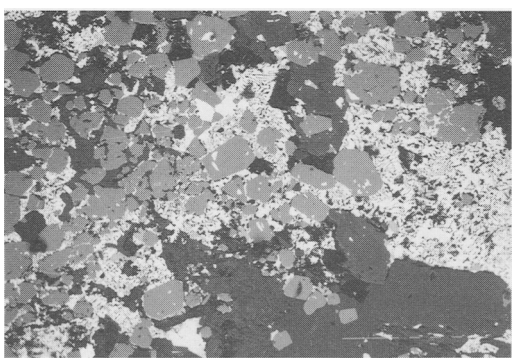

FIG. 7. Backscattered electron image of symplectic intergrowths of sylvanite, calaverite, pezite and goethite (see Fig. 5) enclosing and partially replacing gold (bright white). Width = 550 μm. GCS 17 level, cross-cut 299.

sulphide-bearing vein quartz. Three-phase H_2O–CO_2 inclusions in the dominant milky white quartz accompanying the main core and per-

ipheral telluride mineralization, however, yielded a T_h range of 220–165°C (Fig. 9*b*) with a salinity of approximately 5 wt.% NaCl equiv. and a bulk density of 0.80–0.96 g.cm^{-3}. Three-phase H_2O–CO_2 inclusions in the late altaite–petzite–gold–quartz veinlets (stage IIb) homogenized at temperatures of 175–145°C(Fig. 9*c*) and indicated similar salinities of about 5 wt.% NaCl equiv. but with lower bulk densities of 0.79–0.85 g.cm^{-3}. The late barren quartz–calcite veins (stages III and IV) yielded a T_h range from 220 down to 120°C, the lower temperatures being defined by secondary inclusions (Fig. 9*d*).

Paragenesis

The network of small veins hosting the telluride mineralization in the hangingwall of the main GCS orebody appears to have been generated by hydraulic fracturing and fragmentation of the wallrock during the main mineralizing event at Ashanti. Sulphides, sulpharsenides, sulphosalts (tetrahedrite and bournonite), and an early phase of gold were introduced together with the pale-blue quartz (stage I) which characterizes the GCS orebody. Subsequent reactivation of the Obuasi shear zone led to brittle fracturing of the peripheral blue–grey quartz veins. Synchronous flow of hydrothermal fluid from the main shear zone into these secondary dilatant zones was accompanied by the development of the goethite–hematite–chalcocite–telluride ore of the core mineralization (stage IIa). It is probable that extensive replacement of the earlier sulphide mineralization occurred; the symplectic intergrowth of tellurides and goethite, for example, exhibit evidence for the partial replacement of native gold (Fig. 7). Similarly, the occurrence of copper tellurides with chalcocite and iron oxides, the presence of only relict chalcopyrite, and the complete absence of pyrite, pyrrhotite and arsenopyrite, all suggest that extensive replacement of the early copper and iron sulphides may have occurred. The absence of galena and bournonite may be due to complete replacement by altaite.

The final phase of telluride mineralization, the late gold-rich veinlets (IIb), followed a further period of brecciation and was characterized by the precipitation of altaite, petzite, and gold with no direct evidence of replacement textures. Iron oxides and chalcocite are noticeably absent in these late-stage veinlets.

The mineral assemblages in the ternary Au–Ag–Te system provide some indication of depositional temperatures. The assemblage hessite + sylvanite + petzite is present in the late gold-rich veinlets. Above 170°C, any bulk composition within the hessite + sylvanite + petzite field (Fig. 10) will form a metastable phase which destabilizes at 170°C to the assemblage hessite + petzite + stutzite (Cabri, 1965). Stutzite has not been observed in the late stage gold-rich veinlets and thus a maximum temperature of 170°C is indicated for this last phase of the telluride mineralization.

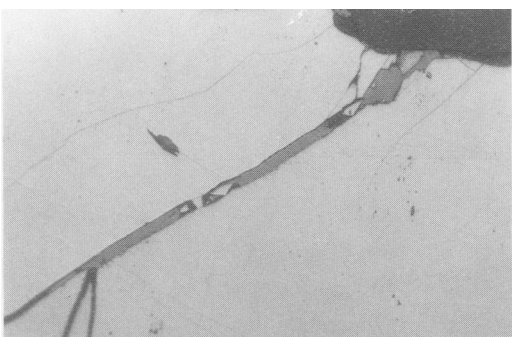

FIG. 8. Photomicrograph of hessite (medium grey) and sylvanite (white) occupying a dilational brittle fracture in a large light grey petzite grain. Field of view = 200 μm across. GCS section, 12.5 level, cross-cut 286.

Discussion

The Ashanti deposit was formed during a major period of deformation and metamorphism related to the *c*.2.0 Ga Eburnian tectonothermal event which appears to have marked the onset of cratonization in West Africa. Fluid-flow was focused along a NNE-trending, crustal-scale shear zone located along the contact between Lower Birimian carbonaceous phyllites and Upper Birimian metavolcanic and pyroclastic rocks (Junner, 1932; Milesi *et al.*, 1988). The steeply dipping shear zone exhibits evidence of both strike–slip and dip–slip displacement. Mesostructural and microstructural evidence clearly demonstrates the synkinematic timing of the multiple phases of hydrothermal activity.

The first phase of the hangingwall mineralization was introduced during the formation of the main Ashanti lodes, and both mineralizations are characterized by quartz, arsenopyrite, pyrite, chalcopyrite, tetrahedrite, galena, bournonite, sphalerite, and gold. However, subsequent brecciation of the early quartz and introduction of the telluride-rich mineralization appears to have been

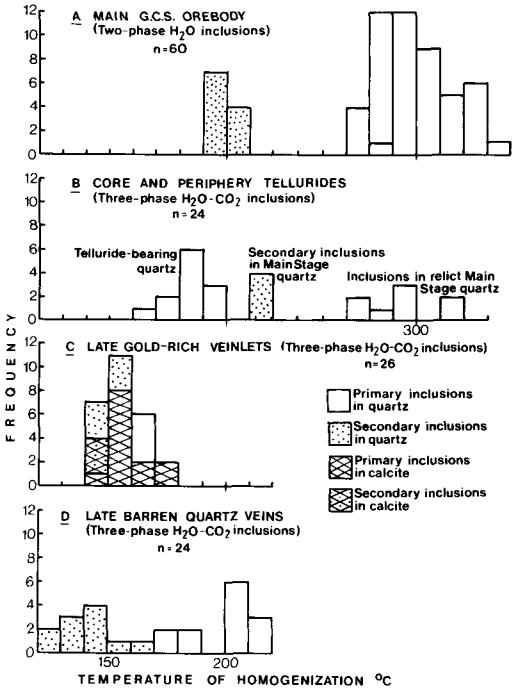

FIG. 9. Fluid inclusion geothermometry of the main Obuasi orebody and hangingwall telluride mineralization; GCS section, 12.5 level, cross-cut 286.

confined to a few hangingwall orebodies. A relatively high f_{O_2} (log f_{O_2}>*c.*−40 bar; see Barton, 1984) is indicated for the tellurium-bearing fluids by the presence of hypogene hematite and goethite in the core mineralization and the absence, perhaps due to replacement, of arsenopyrite and pyrite. The abundance of tellurides and paucity of sulphides, compared to the main-stage Ashanti mineralization, demonstrate a marked increase in the f_{Te_2}/f_{S_2} ratio of the mineralizing fluids, and the occurrence of the copper tellurides in particular confirm the extremely low f_{S_2} of the fluid(s) (Afifi *et al.*, 1988*a*). The absence of ditellurides such as sylvanite ($AuAgTe_4$) and calaverite ($AuTe_2$) in the peripheral assemblages suggests a slightly lower f_{Te_2} in these marginal environments, local variations in telluride mineralogy being a common feature of such deposits (Afifi *et al.*, 1988*b*). Similarly, the abundance of petzite and coarse native gold in the late gold-rich veinlets suggests a late-stage decrease in f_{Te_2}, albeit under low-f_{S_2} conditions. Intriguingly, the low f_{S_2} and the close association between tellurides and marked concentrations of native gold may indicate hydrothermal transport of the gold as telluride or hydrotelluride complexes rather than as hydrosulphide species.

Deposit analogues and crustal setting

Three major types of gold–telluride deposit can be recognized—contact metamorphic, volcanic–hydrothermal, and plutonic–hydrothermal (Twemlow, 1984; see also Markham, 1960; Sindeeva, 1964). The telluride mineralization at Ashanti equate most closely with the plutonic hydrothermal group of deposits.

The plutonic–hydrothermal type are characterized by quartz veins and replacement bodies containing tellurides of Au, Ag, Pb, Hg, and Bi which are usually confined to late fractures within the host quartz. The mineralized lodes are often spatially associated with granodiorite or quartz monzonite intrusions and have a greater vertical continuity than the volcanic type, in some cases extending over intervals of 2000 m or more. These deposits range in age from Archaean to Palaeozoic and Tertiary. Examples from Archaean terranes include the relatively dispersed tellurides of the McIntyre and Hollinger deposits of Ontario (Burrows and Spooner, 1986; Wood *et al.*, 1986), the small but locally very enriched gold–telluride pockets of the Commoner Mine in the Archaean of Zimbabwe (Twemlow, 1984), and the fine-grained calaverite–altaite–coloradoite associated with the gold-rich 'green leader' ore at Kalgoorlie, Western Australia (Nickel, 1977). Important younger examples are the extensive Mesozoic lode systems of the Californian Mother Lode (Knopf, 1929; Weir and Kerrick, 1987).

A particularly complex assemblage of gold, native tellurium, and some fourteen different tellurides has been reported from the Campbell orebody at Bisbee, Arizona (Criddle *et al.*, 1989), where the ore minerals occur in hydrothermally altered breccias and limestone adjacent to a porphyry copper deposit. Telluride mineralization post-dated Sn–W mineralization and appears to represent a style of mineralization intermediate to the plutonic and volcanic types of mineralization.

Despite the plutonic–hydrothermal characteristics of the Ashanti mineralization, the low fluid temperatures imply that the tellurides were introduced during a late stage of thermal decay in the active shear zone. Near-equivalence of homogenization temperatures and temperatures deduced from the telluride phase relations, specifically the absence of stutzite in the late-stage veinlets, indicate that a relatively low fluid pressure persisted, at least during the later stages of the mineralization. Visual estimates of H_2O/CO_2 ratios suggest

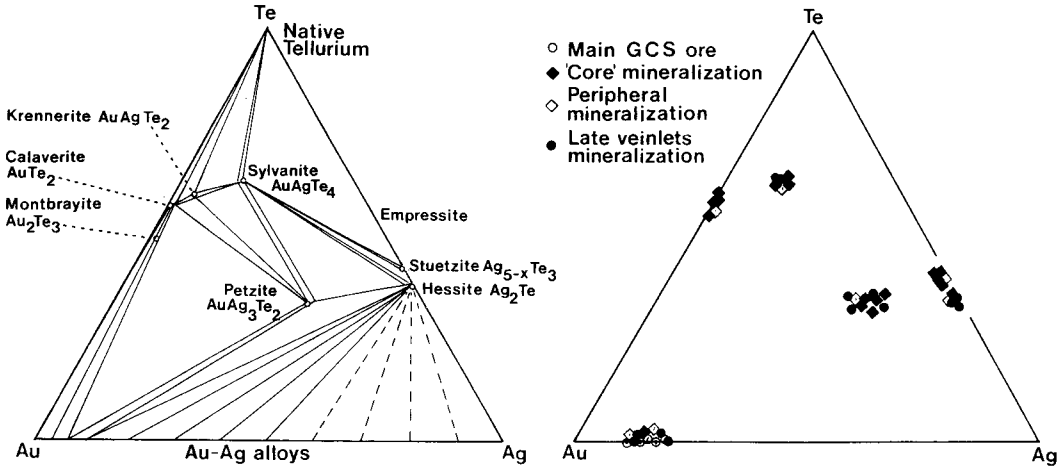

FIG. 10. The system Au–Ag–Te. A: naturally-occurring assemblages (after Twemlow, 1984); B: analytical data for tellurides and gold at Ashanti Mine.

minimum trapping pressures of 0.8 kbar. However, it is not clear whether such low pressures reflect direct uplift and unroofing of the overlying lode or merely a dilation-enhanced decrease in P_f. Thermal impetus for the mineralizing system was probably synkinematic metamorphism, although the presence of synorogenic granitoids in the general vicinity of the Ashanti shear zone may be indicative of some magmatic input. Ready partitioning of tellurium into hydrous phases coexisting with magmas has been postulated by Afifi *et al.* (1988*b*) and could account for a late and time-restricted input of tellurium-rich fluids into the Ashanti shear zone.

An analogue for the Ashanti telluride mineralization with which the authors are familiar is that of the much smaller Commoner Mine in Zimbabwe in which strikingly similar, fracture-controlled mineralization was generated under a very similar thermal regime (Twemlow, 1984; Foster, 1989). In both deposits, very rich zones of gold-telluride mineralization developed as very localized and small pods (up to 20 cm at Ashanti and up to 2 m at Commoner). Clearly, the precipitation mechanisms for gold and tellurium were both specific and highly efficient.

Conclusions

Gold-bearing telluride mineralization at Ashanti was introduced during the later stages of dislocation along a major NE-trending shear zone of early Proterozoic age. The telluride mineralization occurs in the immediate hangingwall of the main gold-sulphide lode, occupying fracture networks within the main-stage quartz. Tellurides and gold were introduced by relatively high f_{O_2}- and high f_{Te_2}/f_{S_2}-fluids which precipitated a complex assemblage of calaverite, sylvanite, kostovite, petzite, hematite and goethite. Precipitation under low f_{S_2} conditions and possible replacement of earlier galena, bornite, pyrite, and chalcopyrite yielded goethite, hematite, altaite, various copper tellurides, and the rare copper–silver telluride henryite. Fluid temperatures for at least a part of the mineralizing event were less than 170°C , and low fluid pressures can be inferred. A magmatic source is tentatively invoked to explain the late injection of a high f_{Te_2}/f_{S_2} fluid into the reactivated shear zone. Precipitation of the tellurides and gold was very efficient, and a greater understanding of the depositional mechanisms would provide an important aid for underground exploration at Ashanti and other mines.

Acknowledgements

Ashanti Goldfields Corporation (Ghana) Ltd is thanked for permitting access to the mine, providing logistic support in Ghana, and allowing publication of the results of the study. Particular thanks are due to the geological staff at Ashanti, namely N. A. Bradshaw, J. A. Amanor, N. d'A. Laffoley, and A. J. Rex for their assistance and hospitality and for their comments on an early draft of this paper. Comments on the manuscript by A. J. Criddle, R. A. D. Pattrick, J. F. W. Bowles, and an anonymous reviewer are also warmly acknowledged. RJB is supported by a Natural Environment Research Council CASE studentship in collaboration with AGC (Ghana) Ltd.

References

Afifi, A. M., Kelly, W. C., and Essene, E. J. (1988*a*) Phase relations among tellurides, sulfides and oxides: I Thermochemical data and calculated equilibria. *Econ. Geol.* **83**, 377–94.

—— —— —— (1988*b*). Phase relations among tellurides, sulfides and oxides: II Applications to telluride-bearing ore deposits. Ibid., 395–404.

Amanor, J. (1979) *The geology of Ashanti gold mines and implications for exploration.* MSc thesis (unpubl.), Imperial College, London.

—— Bradshaw, N. G., Gyapong, W. A., Miller, J. F. G., and Sinclair, C. (1978) *The geology of the Ashanti Goldfields.* Unpub. rep., Ashanti Goldfields Corporation (Ghana) Ltd.

Barton, P. B. (1984) Redox reactions in hydrothermal fluids. In *Fluid–Mineral Equilibria in Hydrothermal Systems* (Henley, R. W., Truesdall, A. H., and Barton, P. B., eds.). Soc. Econ. Geol. 99–113.

Burrows, D. R. and Spooner, E. T. C. (1986) The McIntyre Cu–Au deposit, Timmins, Ontario, Canada. In *Proceedings of Gold '86: an International Symposium on the Geology of Gold'* (Macdonald, A. J., ed.) Toronto, 23–40.

Cabri, L. J. (1965) Phase relations in the Au–Ag–Te system and their mineralogical significance. *Econ. Geol.* **60**, 1569–606.

Cappendell, G. (1987) Ashanti. *Mining Magazine*, August, 122–9.

Criddle, A. J., Stanley, C. J., Chisholm, J. E., and Fejer, E. E. (1983) Henryite, a new copper–silver telluride from Bisbee, Arizona. *Bull. Mineral.* **106**, 511–7.

—— —— and Eady, C. S. (1989) Ore mineralogy and mineralization of the Campbell orebody, Bisbee, Arizona. *Int. Geol. Congress, abstracts*, Washington, **1**, 340–1.

Foster, R. P. (1989) Archaean Gold Mineralization in Zimbabwe: Implications for Metallogenesis and Exploration. In *The Geology of Gold Deposits: the Perspective in 1988.* Econ. Geol. Monograph 6, Econ. Geol. Publ. Co., 54–70.

Gyapong, W. A. (1980) *Factors controlling ore localization at Ashanti Mine, Ghana.* MSc. thesis (unpubl.), Imperial College, London.

Harding, T. P. (1985). Seismic characteristics and identification of negative flower structures, positive flower structures and positive structural inversion. *Am. Assoc. Petrol. Geol.* **69**, 582–600.

Hirdes, W., Leube, A., Mawer, R., and Kesse, G. O. (1988*a*) The Birimian Supergroup of Ghana: Depositional environment, tectonothermal development and conceptual model of an early Proterozoic suite (extend. abs.). *International Conference and Workshop on the Geology of Ghana with Special Emphasis on Gold. Geology and exploration in Ghana and in selected other Precambrian terrains.* Accra, Ghana 9–16th Oct 1988, Programme and Abstracts, 17–18.

—— Saager, R., and Leube, A. (1988*b*) New structural, radiometric and mineralogical aspects of the Au-bearing Tarkwaian group of Ghana. In *Bicentennial Gold '88.* Extend. abs. poster programme, Vol. 1. 146–8.

Junner, N. R. (1932) *The geology of the Obuasi Goldfield.* Memoir Gold Coast Geological Survey, No 2, 65pp.

Kesse, G. O. (1984) The occurrence of gold in Ghana, In *Gold '82: Geochemistry and Genesis of Gold Deposits* (Foster R. P., ed.). A. A. Balkema, Rotterdam, 645–59.

—— (1985) *The Mineral and Rock Resources of Ghana.* A.A. Balkema, Rotterdam, 610pp.

Knopf, A. (1929) *The Mother Lode system of California.* U.S. Geol. Surv., Prof. Paper 157, 88p.

Leube, A., Hirdes, W., Mauer, R., and Kesse, G. O. (1990) The early Proterozoic Birimian Supergroup of Ghana and some aspects of its associated gold mineralization. *Precamb. Res.* **46**, 139–65.

Markham, N. L. (1960) Synthetic and natural phases in the system Au–Ag–Te. *Econ. Geol.* **55**, 1148–78.

Milesi, J. P., Ledru, P., Ankrah, P. T., Marcoux, E., Vinchon, C. and Johan, V. (1988) Geological and structural setting of the Ghana Gold Deposits hosted by Birimian formations (extend. abs.). *International Conference and Workshop on the Geology of Ghana with Special Emphasis on Gold: Geology and exploration in Ghana and in selected other Precambrian terrains.* Accra, Ghana 9–16th Oct 1988, Programme and Abstracts, 31–32.

Nickel, E. (1977) Mineralogy of the 'Green Leader' gold ore at Kalgoorlie, Western Australia. *Proc. Aust. Inst, Min. Met.* **263**, 9–13.

Sindeeva, N. D. (1964) *Mineralogy and Types of Deposits of Selenium and Tellurium.* John Wiley, New York, 363pp.

Suttill, K. R. (1989) Ghana's golden glow. *Eng. Min. Journal*, June, 22–33.

Twemlow, S. G. (1984) Archaean gold-telluride mineralization of the Commoner Mine, Zimbabwe. In *Gold '82: the Geology, Geochemistry and Genesis of Gold Deposits* (Foster, R. P., ed.), A. A. Balkema, Rotterdam, 469–92.

Weir, R. H. Jr., and Kerrick, D. M. (1987) Mineralogical, fluid inclusion and stable isotope studies of several gold mines in the Mother Lode, Tuolumne and Mariposa Counties, California. *Econ. Geol.* **82**, 328–44.

Wilson I. R. (1972*a*) Carbonaceous matter in wallrock, Ashanti gold mine, Obuasi, Ghana. *14th Ann. Rep. Res. Inst. African Geol.*, Univ, Leeds, 33–4.

—— (1972*b*) *Wallrock alteration at Geevor Mine, Cornwall and Ashanti Mine, Ghana.* PhD thesis (unpubl.), Univ. of Leeds.

Wood, P. C., Burrows, D. R., Thomas, A. V. and Spooner, E. T. C. (1986) The Hollinger–McIntyre Au–quartz vein system, Timmins, Ontario, Canada; geologic characteristics, fluid properties and light stable isotope geochemistry. In *Proceedings of Gold '86, an International Symposium on the Geology of Gold* (Macdonald, A. J., ed.), Toronto, 56–81.

Wright, J. B., Hastings, D. A., Jones, W. B., and Williams, H. R. (1985) *Geology and Mineral Resources of West Africa.* George Allen & Unwin, London, 187pp.

[*Manuscript received 19 January 1990; revised 27 April 1990*]